SLAC-PUB-541 (Revised)
January 1969
(TH) & (EXP)

PHOTOPRODUCTION OF RHO MESONS FROM COMPLEX NUCLEI AT 9 BeV*

F. Bulos, W. Busza, R. Giese, R. R. Larsen,
D. W. G. S. Leith, and B. Richter

Stanford Linear Accelerator Center
Stanford University, Stanford, California

V. Perez-Mendez, A. Stetz and S. H. Williams

Lawrence Radiation Laboratory
University of California, Berkeley, California

and

M. Beniston and J. Rettberg

IBM Scientific Center
Palo Alto, California

ABSTRACT

We have measured the absolute differential cross section for photoproduction of neutral rho mesons from complex nuclei at a photon energy of 8.8 BeV. Using a two-parameter optical model, we have deduced a value for the total rho-nucleon cross section of $(30 \pm \frac{6}{4})$ mb. Application of the Vector Dominance Model results in a value for the rho photon coupling of $\gamma_\rho^2/4\pi = 1.1 \pm 0.2$.

Note: A shorter version of this paper appeared in Phys. Rev. Letters 22, 490-493 (1969).

*Work supported by the U. S. Atomic Energy Commission.

We report here the results of a measurement of the photoproduction of pion pairs from complex nuclei at 8.8 BeV. These results are part of a systematic study of rho meson photoproduction from a variety of targets, (H_2 through Pb), in the energy range of 5-16 BeV. Similar experiments performed at 2 to 6 BeV[1-4] have produced disparate results when interpreted within the framework of the Vector Dominance Model (VDM).[5] Since the VDM has successfully correlated many phenomena, it is of interest to study the limits of its applicability and to resolve any theoretical or experimental inconsistencies that arise. A preliminary report of this data has been presented elsewhere.[6]

The experiment was performed in the SLAC monochromatic photon beam using a wire spark chamber spectrometer which was on-line to an IBM 1800 computer. Figure 1 illustrates the spectrometer. The organization of the on-line computing system is described elsewhere.[7] The properties of the beam and the measurement of the spectrum are also described elsewhere.[8] The energy of the monochromatic peak was 8.85 ± 0.02 BeV with a FWHM of 0.52 BeV. To calibrate the absolute photon flux, the spark chamber system was periodically used as a pair spectrometer. The system had a mass acceptance of ~1000 MeV at any given setting, with a maximum detectable mass of ~3500 MeV. The mass resolution varied from ± 6 MeV at 700 MeV to ± 15 MeV at 3000 MeV. The momentum transfer acceptance ranged from 0 to 0.25 $(BeV/c)^2$, with a resolution of ~0.0005 $(BeV/c)^2$ for small t, and increasing to 0.002 $(BeV/c)^2$ for large t. The apparatus detected meson decays over 80% of the decay solid angle at 9 BeV.

Data was taken using targets of Be, C, Al, Cu, Ag and Pb, ranging in thickness from 0.1 rℓ for Be to 0.3 rℓ for Pb. The target position was set to maximize the spectrometer acceptance for pion pairs with energy comparable to the energy of the monochromatic photons and mass in the vicinity of the rho. Electromagnetic attenuation of the photons and absorption of pion pairs were measured by varying the thickness of the Be target; the results were in agreement with calculations and these calculated

corrections (12%) were applied to the data from all other elements. Other corrections, measured and calculated, include: target - out yield (2%), track finding inefficiency (8%), pion decay (2%), pions grazing the edges of the beam stopper (2%), and dead time (<1%). The total correction factor varies from 1.26 ± .06 for Be to 1.35 ± 0.09 for Pb.

The energy spectrum of the pion pairs from Be is shown in Fig. 2a. We have verified that the pion-pair yield is independent of the size of the energy cut for cuts less than ± 0.75 BeV centered around 8.8 BeV. This, together with the observation that the pion pair spectrum and photon spectrum[8] are very similar, is a strong indication that we have a negligible contribution from inelastic events. The events included in the cross section determinations were those with an energy between 8.4 and 9.5 BeV. The observed di-pion mass spectrum from Be, corrected for the spectrometer acceptance, (Fig. 2b) is similar to that observed in other photoproduction experiments.[1-4,9] The observed distributions for each element were modified to include the fact that the minimum momentum transfer, $t_{min} = -(M_{\pi\pi}^2/2k)^2$, tends to suppress large masses, particularly for the heavy elements which have rapidly falling form factors. This correction is small at 8.8 BeV but is very serious for lower photon energies. The number of events N per unit mass $M_{\pi\pi}$ was fitted to

$$\frac{dN}{dM_{\pi\pi}} = C_0 M_\rho \left[\frac{M_{\pi\pi}\Gamma}{(M_\rho^2 - M_{\pi\pi}^2)^2 + M_\rho^2\Gamma^2} + C_1 \frac{M_\rho^2 - M_{\pi\pi}^2}{(M_\rho^2 - M_{\pi\pi}^2)^2 + M_\rho^2\Gamma^2} + C_2 \right] \qquad (1)$$

with

$$\Gamma = \Gamma_\rho \cdot \frac{M_\rho}{M_{\pi\pi}} \cdot \left(\frac{M_{\pi\pi}^2 - 4\mu^2}{M_\rho^2 - 4\mu^2} \right)^{3/2}$$

where $\mu = 0.139$ BeV, and C_0, C_1, C_2, M_ρ, Γ_ρ were allowed to vary. The first term in (1) is the ordinary p-wave Breit Wigner, and the second term represents the interference with a coherent background which might arise from a process[10] in which one of the pions diffractively scatters off the nucleus. This interference has been proposed

by Söding[11] as a possible explanation of the observed differences in rho production by pions and photons. We find our best fit (χ^2 per degree of freedom 1.26) to be M_ρ = 767 ± 4 MeV and Γ_ρ = 142 ± 7 MeV. According to our fit the background diffractive amplitude is so small that only the interference term is appreciable. The subsequent analysis includes only those events with masses in the range 650 to 850 MeV. This mass region accounts for 63% of the rhos contained in a p-wave Breit Wigner normalized to unity with the s-wave normalization constant.[12] We have also fitted the data to a Breit Wigner multiplied by $(M_\rho/M_{\pi\pi})^4$, as proposed by Ross and Stodolsky,[13] plus a polynomial background. We find an acceptable fit with M_ρ = 761 ± 3 MeV and Γ = 131 ± 8 MeV. The determination of the cross-section is insensitive, within our quoted accuacy, to the type of fit used.

The momentum transfer distribution of the events surviving the energy and mass cut, and a cut in the decay angle, θ_d, given by $|\cos\theta_d| \leq 0.5$, are shown in Figs. 3a - 3f. The differential cross sections are also tabulated in Tables Ia - If. This data clearly shows the rapidly falling contribution from coherent production and an underlying incoherent contribution. In order to determine the forward ($t = t_{min}$) value of the differential cross section, the data in the diffraction peak was fitted to an optical model, which included both a coherent contribution, and an incoherent part that vanished in the forward direction; a hard sphere nuclear density of radius $R=r_0A^{1/3}$ was used, and r_0 was allowed to vary for each element. The values of r_0 obtained in this way, are listed in Table II. They show a definite decrease with increasing A. This A-dependence is a consequence of the well known inadequancy of the hard-sphere approximation to the nuclear density; in fact, our own values of r_0 are consistent with the electromagnetic "equivalent hard-sphere" radii.[14] We emphasize that the hard-sphere model was only used to smooth the data and to obtain the forward cross section. The corrected forward cross sections, listed in Table II, may now be used to determine the total rho-nucleon cross section, $\sigma_{\rho N}$, and the photon-rho coupling constant for zero mass rho mesons.[15]

The photoproduction of rho mesons from nuclei is related to the photoproduction from single nucleons and to the nuclear absorption of rhos as they emerge from the nuclear matter (i.e., $\sigma_{\rho N}$). The explicit relation[16] based on an optical model of the nucleus is

$$\frac{d\sigma}{dt}(\gamma A \rightarrow \rho^{o} A) = \frac{d\sigma}{dt}(\gamma N \rightarrow \rho N)\, f\left(\sigma_{\rho N}, \rho(r), t\right) \qquad (2)$$

where

$$f(\sigma_{\rho N}, \rho(r), t) = \left| 2\pi \int_{0}^{\infty}\int_{-\infty}^{\infty} b\,db\,dz\, J_{0}(q_{\perp} b)\, \rho(b,z)\, e^{i\sqrt{-t_{min}}\, z - \frac{\sigma_{\rho N}}{2}\int_{z}^{\infty} \rho(b,z')dz'} \right|^{2} \qquad (3)$$

where b and z are nuclear coordinates, $q_{\perp}$ is the transverse momentum transfer, and $\rho(r)$ is the nucleon density. We use the Wood-Saxon $\rho(r)$

$$\rho(r) = \rho_{0}\left(1 + e^{\frac{r-c}{a}}\right)^{-1} \qquad (4)$$

because it successfully describes electron-nuclear scattering[14] over a wide range of A with only two parameters; a half-density radius $C = C_{0}A^{1/3} = 1.08\ A^{1/3}$ fermi, and a surface parameter a = 0.535 fermi. We have performed our analysis using C_{0} = 1.08 and 1.18 fermi. These values represent our estimates for the limits on the nuclear radii in hadronic interactions and include the "hard-sphere" radii determined in this experiment (see Table II) We will discuss the results obtained with C_{0} = 1.18 fermi; results based on the electromagnetic radii are shown in Table II and Fig. 4c. The value of C_{0} may however, be a function of A, changing ~15% between Pb and Be.[17] This would increase our estimate of $\sigma_{\rho N}$ ~15%. This effect is included in our estimate of the systematic errors.

The A-dependence of the forward ($t = t_{min}$) cross sections depend only on $\sigma_{\rho N}$ for a given nuclear density. The measured forward cross sections, relative to Cu, are shown in Fig. 4a. Taking the relative cross sections avoids, in this part of the analysis, assumptions about the details of the ρ photoproduction amplitude and utilizes

only the A-dependence predicted by the optical model. The solid line is the best fit to our data using Eq. (2), from which we deduce that $\sigma_{\rho N} = 31 \pm 4$ mb. Our measured relative A-dependence is in good agreement with that of McClellan et al.;[4] in fact, a reanalysis of their data, using the method described above yields $\sigma_{\rho N} = 30$ mb. The difference between this and their quoted value of $\sigma_{\rho N} = 38.5 \pm 4.5$ is due to the different nuclear densities used. We are unable to make a similar comparison with the data of Asbury et al.[2] because the calculations are so sensitive[18] to the model at low energies. Their quoted value is $\sigma_{\rho N} = 31.3 \pm 2.3$ mb.

Having deduced the value of $\sigma_{\rho N}$, we can use the vector dominance model of photon-hadron interactions to determine the value of the coupling constant. The VDM together with the optical theorem leads to:

$$\left.\frac{d\sigma}{dt}\right|_{t_{min}} (\gamma A \rightarrow \rho A) = \frac{\alpha}{4}\left(\frac{4\pi}{\gamma_\rho^2}\right) \frac{\sigma_{\rho N}^2}{16\pi} \cdot f(\sigma_{\rho N}, t_{min}) \qquad (5)$$

assuming that ρN scattering amplitude is imaginary.

The value of $\gamma_\rho^2/4\pi$ was calculated for each target nucleus using our data and our $\sigma_{\rho N}$. The results are listed in Table II and shown in Fig. 4b. The solid line is the best A-independent fit to our data, and gives $\gamma_\rho^2/4\pi = 1.21 \pm 0.05$ (statistical error). This is in strong disagreement with the value quoted by Asbury et al., $(0.45 \pm .1)$; the difference (a factor of 2.5) is due either to the absolute normalization of the cross section data or to the difficulty of extrapolation at low energies.[18] On the other hand, our value appears to be in very good agreement with that of McClellan et al;[4] the precision of the agreement is due to the somewhat fortuitous cancellation of the different absolute normalization (20%) and different $\sigma_{\rho N}$(~15%). However, it must be emphasized that these two experiments do agree to within 20% on a value of $\gamma_\rho^2/4\pi$ about 1.0 and are incompatible with a value of 0.5

To display more graphically the implicit relation of $\gamma_\rho^2/4\pi$ and $\sigma_{\rho N}$ and to demonstrate the sensitivity of these deductions, we plot in Fig. 4c this relation, (5), for several

complex nuclei using our measured cross sections. The two points located in the overlap region are our best solutions for the limiting radii. The widths of the bands represent the uncertainty in $\gamma_\rho^2/4\pi$ due to lack of knowledge of nuclear radii. The figure also dramatically demonstrates that the determination of $\gamma_\rho^2/4\pi$ becomes less sensitive to $\sigma_{\rho N}$ as A increases and nuclei becomes more opaque; in fact, for Pb, a ± 5 mb change in a 30 mb $\sigma_{\rho N}$ leads to a $\pm 14\%$ change in $\gamma_\rho^2/4\pi$. In contrast, a precise measurement of the forward cross section for hydrogen does not result in a precise determination of $\gamma_\rho^2/4\pi$ because of the intrinsic difficulties in the measurement of $\sigma_{\rho N}$, caused by uncertaintes in the nuclear density.

Taking the average of our values of $\sigma_{\rho N}$ and $\gamma_\rho^2/4\pi$ based on the limiting radii, we obtain $\sigma_{\rho N} = 30 \pm {}^{6}_{4}$ mb and $\gamma_\rho^2/4\pi = 1.1 \pm 0.2$, where the errors include contributions from statistics, normalization of photon flux, and an uncertainty attributed to the optical model and nuclear density.

We observe that: (1) There are now two determinations of $\gamma_\rho^2/4\pi \approx 1.0$ from the reaction $\gamma + A \rightarrow \rho^o + A$; (2) a proper evaluation of $\gamma_\rho^2/4\pi$ using the measured branching ratio[20] for $\omega \rightarrow \pi^o + \gamma$[21] and $\Gamma_\rho = 111 \pm 6$ MeV[19] yields $\gamma_\rho^2/4\pi = 0.9 \, {}^{+.06}_{-.12}$; (3) there is a large disparity observed in the comparison[22] of polarized photoproduction of pions with rho production by pions; (4) nucleon isovector form factors are not compatible with a single rho pole; (5) the determinations of $\gamma_\rho^2/4\pi$ from a study of $e^+e^- \rightarrow \pi^+\pi^-$[19] and leptonic decays[19] (i.e. photons on the rho mass shell) yields a value of 0.52 ± 0.03. These observations directly confront the validity of simple rho dominance and may imply a q^2 dependence to the $\gamma\rho$ coupling and/or contributions from higher vector mesons. A more thorough comparison of theory and experiment is in progress.

ACKNOWLEDGMENTS

We gratefully acknowledge the assistance of G. Chadwick, R. Diebold, J. Good, A. Kilert, R. Russell and H. H. Williams in the design, construction, execution and analysis of the experiment. Numerous discussions with Dr. R. Diebold, Dr. F. Gilman and Prof. D. Ritson have been most valuable.

REFERENCES

1. L. J. Lanzerotti, et al., Phys. Rev. 166, 1365 (1968).
2. J. G. Asbury, et al., Phys. Rev. Letters 19, 865 (1967); J. B. Asbury, et al., Phys. Rev. Letters 20, 227 (1968).
3. H. Bleckschmidt, et al., Nuovo Cimento 52A, 1348 (1967).
4. G. McClellan, et al., Preprints CLNS-41,44, Lab. Nuc. Studies, Cornell University, Ithaca, N. Y. (Dec. 1968) and submitted to Phys. Rev. Letters.
5. J. J. Sakurai, Ann. of Phys. (N.Y.) 11, 1 (1960); N. M. Kroll, T. D. Lee, B. Zumino, Phys. Rev. 157, 1376 (1967).
6. F. Bulos, et al., "Photoproduction of Rho Mesons at 9 BeV", Proc. of the XIVth Int. Conf. on High Energy Physics, Vienna, (Sept. 1968).
7. M. Beniston, "On Line Analysis of Wire Spark Chamber Data", and R. Russell, "On-Line Wire Spark Chamber Data Acquisition System", presented at the XVth IEEE Nuc. Sci. Sym., Montreal, (Oct. 1968); F. Bulos, et al., Proc. of the Int. Symp. on Nuc. Elec. and Inst. for High Energy Physics, Versailles, (Sept. 1968).
8. J. Ballam, et al., "The SLAC Monochromatic Photon Beam", Report No. SLAC-PUB-530, Stanford Linear Accelerator Center, Stanford, California, (Dec. 1968).
9. German Bubble Chamber Collaboration, N. C. 46, 795 (1966) and N. C. 48, 262 (1967); Cambridge Bubble Chamber Group, Phys. Rev. 146, 994 (1966); Brown-Harvard-MIT-Padova-Weizmann Institute Bubble Chamber Group, Phys. Rev. 155, 1468 (1967).
10. S. D. Drell, Phys. Rev. Letters 5, 278 (1960).
11. P. Söding, Phys. Rev. Letters. 19, 702 (1966).

12. This normalization constant is

$$\left[\frac{\pi}{2} - \tan^{-1}\left[\frac{4\mu^2 - M_0^2}{\Gamma_0 M_0}\right]\right]^{-1} = \frac{1.07}{\pi}$$

In the limit $\Gamma_0/M_0 << 1$, this becomes $\frac{1}{\pi}$, the normalization used by McClellan et al.

13. M. Ross, L. Stodolsky, Phys. Rev. 149, 1172 (1966).

14. R. Hofstadter, Ann. Rev. Nucl. Sci., 4, 231 (1957); H. R. Collard, L. R. B. Elton, R. Hofstadter, Landolt-Bornstein, New Series Vol. 2, Nuclear Radii, (1967).

15. We define the photon-rho coupling constant to be $em_\rho^2/2\gamma_\rho$.

16. S. D. Drell, J. S. Trefil, Phys. Rev. Letters 16, 552 (1966); K. S. Kolbig, B. Margolis, Nucl. Phys. B6, 85 (1968).

17. R. G. Glauber, G. Matthiae, Report ISS. 67/16, Istituto Superiore di Sanita, Rome, Italy.

18. For the photon energies 2.7, 4.5 and 9 BeV the extrapolation factors on Pb are 19, 2.7, 1.3 and for Be are 2, 1.3, 1.1.

19. Orsay Storage Ring Group, Report LAL-1204, (Nov. 1968), Linear Accelerator Laboratory, Orsay, France; S. C. C. Ting, Proc. of the XIVth Int. Conf. on High Energy Phys, Vienna, (1968); V. L. Auslender, et al., Institut Yadernoi Fiziki, Akad. Nauk SSSR, Preprint 243, Novosibirsk (1968).

20. Particle Data Group, UCRL-8030 Pt. 1, Aug. (1968) Rev.

21. M. Gell-Mann, D. Sharp, W. G. Wagner, Phys. Rev. Letters 8, 261 (1962).

22. R. Diebold, J. A. Poirier, SLAC PUB-534, Stanford Linear Accelerator Center, Stanford University, Stanford, California (1968).

Table I: Measured Differential Cross Sections For

$\gamma + A \longrightarrow \rho^{o} + A$ at $E_{\gamma} = 8.8$ BeV

Ia Beryllium			Ib Carbon		
-t	$\frac{d\sigma}{dt}$ (BeV/c)^2	statistical error	-t	$\frac{d\sigma}{dt}$ (BeV/c)^2	statistical error
.003	2.95	.45	.003	6.78	1.29
.005	2.99	.43	.005	7.54	1.40
.007	3.16	.46	.008	3.54	.68
.009	2.40	.40	.012	3.68	.70
.012	2.23	.29	.016	3.59	.69
.016	1.59	.24	.020	2.05	.54
.020	1.56	.25	.026	1.87	.40
.024	1.09	.21	.034	.84	.29
.028	1.25	.23	.042	.79	.29
.032	.59	.16	.054	.82	.21
.036	.91	.20	.094	.18	.07
.040	.71	.19			
.044	.77	.20			
.050	.37	.10			
.058	.40	.11			
.066	.34	.13			
.078	.35	.09			
.102	.09	.04			
.50	.10	.05			

Table I cont'd.

Ic Aluminum			Id Copper		
-t	$\frac{d\sigma}{dt}$ (BeV/c)^2	statistical error	-t	$\frac{d\sigma}{dt}$ (BeV/c)^2	statistical error
.002	24.1	3.4	.002	82.1	10.2
.004	22.8	3.4	.004	61.0	8.9
.006	13.8	2.6	.006	52.4	8.4
.008	16.3	2.8	.008	34.8	7.1
.010	9.8	2.1	.011	19.6	3.6
.012	10.5	2.3	.015	12.7	3.0
.014	10.4	2.5	.021	5.7	1.4
.016	8.6	2.3	.033	1.5	0.6
.019	3.4	1.0	.049	0.7	0.4
.023	3.6	1.1	.065	1.4	0.7
.029	2.2	0.6			
.041	0.8	0.3			
.057	0.9	0.3			
Ie Silver			If Lead		
.002	118.	25.	.0015	287.	60.
.004	101.	25.	.0025	370.	70.
.006	82.	22.	.0035	301.	67.
.009	38.	11.	.0045	216.	52.
.019	5.	2.	.006	131.	30.
.043	2.5	1.4	.008	62.	23.
			.011	42.	14.
			.017	12.	5.
			.029	5.	3.

TABLE II

The forward cross sections, the extrapolated t = 0 cross sections (using $\sigma_{\rho n}$ = 30 mb and C_0 = 1.18), the equivalent "hard sphere" radii and the photon-rho coupling constant determined in this experiment are listed below.

A	Events (unweighted)	$\left.\frac{d\sigma}{dt}\right\|_{t_{min}}$ (mb/(BeV/c)^2)	$\left.\frac{d\sigma}{dt}\right\|_{t=0}$ (mb/(BeV/c)^2)	Radius $r_0 = RA^{-\frac{1}{3}}$	$\gamma_\rho^2/4\pi$ for C_0 = 1.08	$\gamma_\rho^2/4\pi$ for C_0 = 1.18
Beryllium$^{(9)}$	549	3.48 ± .27	3.73 ± .29	1.35 ± .09	1.08 ± .08	1.37 ± .1
Carbon$^{(12)}$	229	6.85 ± .74	7.39 ± .80	1.40 ± .14	0.89 ± .10	1.14 ± .12
Aluminum$^{(27)}$	316	26.7 ± 2.7	29.6 ± 3.0	1.35 ± .08	0.87 ± .09	1.11 ± .11
Copper$^{(64)}$	278	90.4 ± 9.2	104.7 ± 10.2	1.17 ± .05	0.98 ± .10	1.26 ± .12
Silver$^{(108)}$	82	147 ± 29	178 ± 35	1.10 ± .12	1.30 ± .26	1.68 ± .33
Lead$^{(208)}$	123	525 ± 69	677 ± 89	1.16 ± .08	0.91 ± .12	1.18 ± .15
					0.97 ± 0.04	1.23 ± .05

FIGURE CAPTIONS

1. The spectrometer system, showing the arrangement of the counters, the magneto-strictive read-out wire spark chambers and the two photon monitors; a pair spectrometer and a shower counter inside the tungsten beam stopper. Periodically, for calibrating the 2D4 pair spectrometer, the beam stopper was removed and the spark chamber system converted into an electron-positron pair spectrometer.

2. a) The energy spectrum of $\pi^+\pi^-$ pairs detected by the wire chamber spectrometer, showing the monochromatic peak at 8.8 BeV;

   b) the mass distribution of pion pairs produced from Be by photons from the monochromatic peak. The solid line is the best fit to the data using a coherent mixture of resonant and diffractive background amplitudes (see text).

3. The differential cross sections for the process $\gamma A \longrightarrow \rho^0 A$ at 8.8 BeV.

4. a) The forward cross section as a function of A, relative to Cu. The solid line is the best fit using the optical model described in the text with $C_0 = 1.18$ fermi; the $\sigma_{\rho N}$ deduced from this fit is (31 ± 4) mb. (Statistical error.)

   b) The photon-rho coupling constant as determined from our forward cross sections and $\sigma_{\rho N}$. The solid line is the best A-independent fit to the data and gives $\gamma_\rho^2/4\pi = 1.21 \pm 0.05$. (Statistical error.)

   c) The dependence of $\gamma_\rho^2/4\pi$ on $\sigma_{\rho N}$ for our measured forward cross sections for several nuclei. In the relation $\sigma_{\rho N}$ is in barns and $d\sigma/dt$ in mb/(BeV c)^2. The two points are our best value of $\gamma_\rho^2/4\pi$ and $\sigma_\rho N$ determined as illustrated in Fig. 2a and 2b.

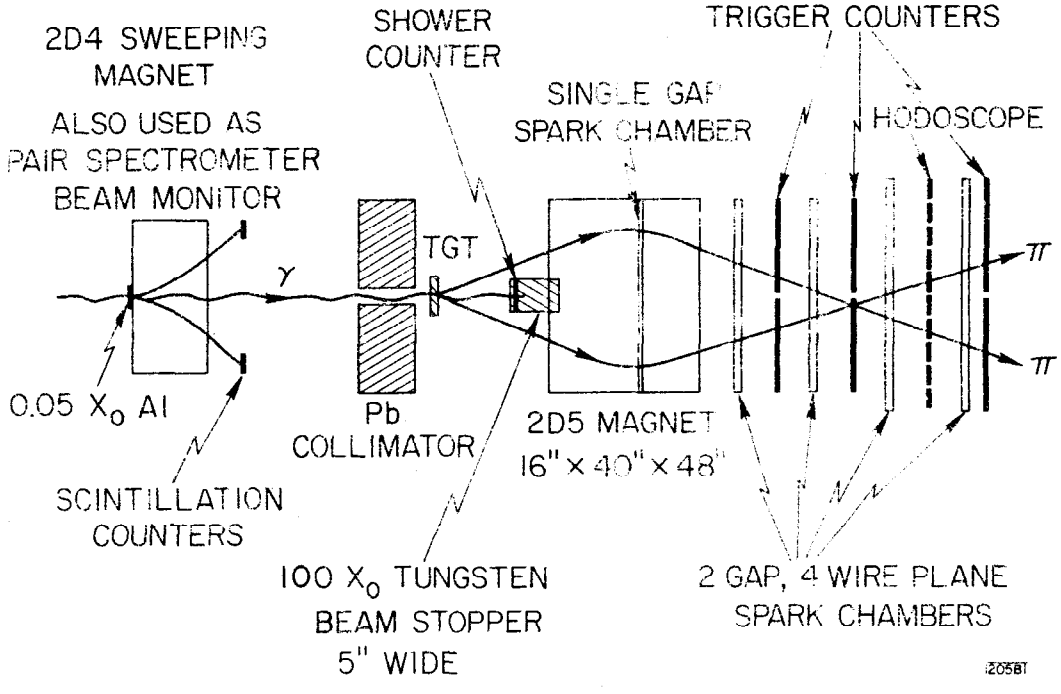
2D4 SWEEPING MAGNET
ALSO USED AS PAIR SPECTROMETER BEAM MONITOR
SHOWER COUNTER
SINGLE GAP SPARK CHAMBER
TRIGGER COUNTERS
HODOSCOPE
TGT
γ
π
π
0.05 X0 Al
SCINTILLATION COUNTERS
Pb COLLIMATOR
2D5 MAGNET
16" × 40" × 48"
100 X0 TUNGSTEN BEAM STOPPER 5" WIDE
2 GAP, 4 WIRE PLANE SPARK CHAMBERS
2058T

Fig. 1

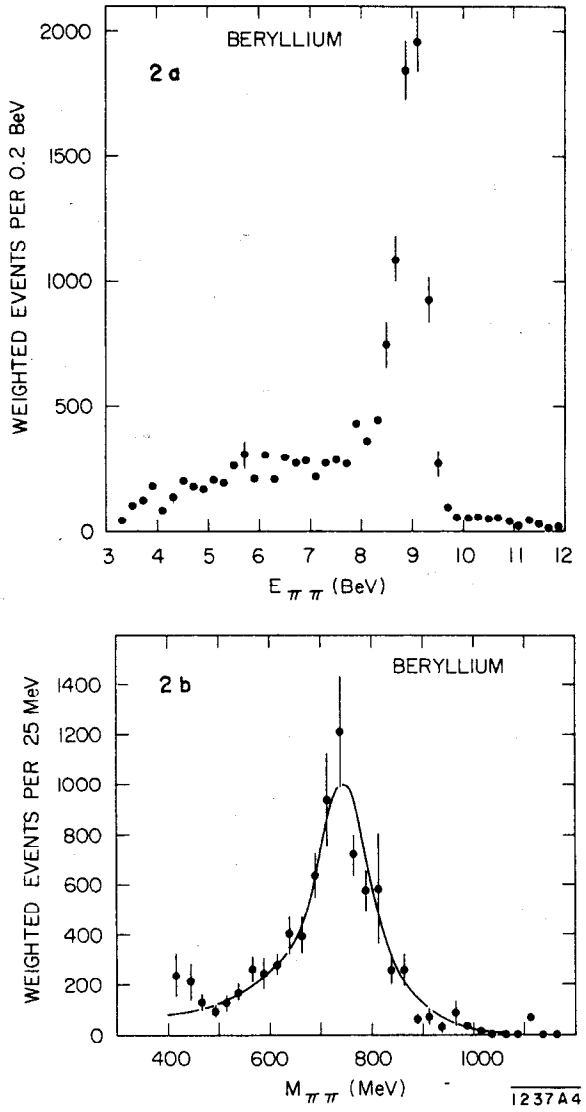
BERYLLIUM
2 a
WEIGHTED EVENTS PER 0.2 BeV
2000
1500
1000
500
0
3
4
5
6
7
8
9
10
11
12
$E_{\pi\pi}$ (BeV)
BERYLLIUM
2 b
WEIGHTED EVENTS PER 25 MeV
1400
1200
1000
800
600
400
200
0
400
600
800
1000
$M_{\pi\pi}$ (MeV)
1237A4

Fig. 2

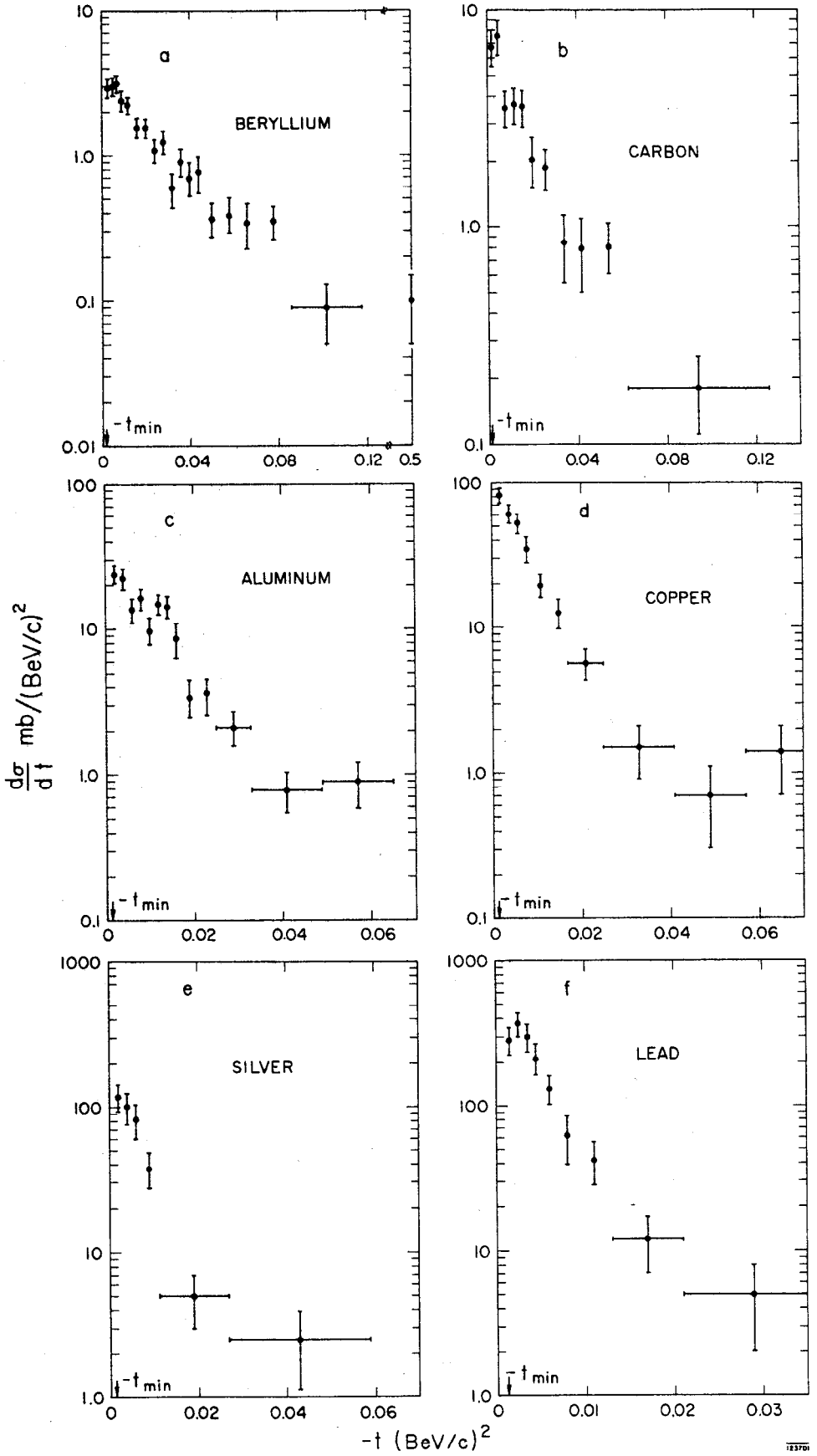
a
BERYLLIUM
b
CARBON
c
ALUMINUM
d
COPPER
e
SILVER
f
LEAD
$-t_{min}$
$\frac{d\sigma}{dt}$ mb/(BeV/c)^2
$-t$ (BeV/c)^2

Fig. 3

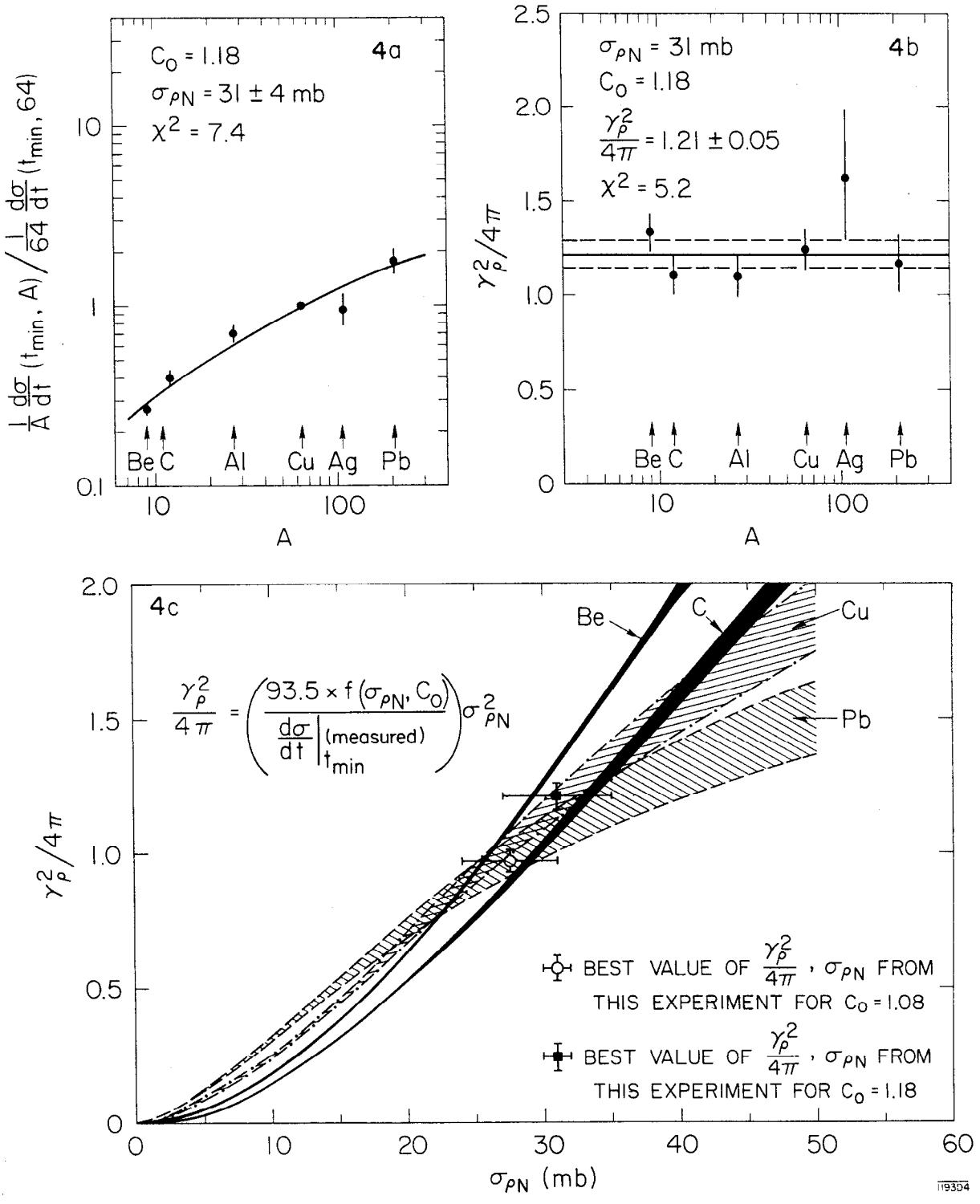
4a
$C_0 = 1.18$
$\sigma_{\rho N} = 31 \pm 4$ mb
$\chi^2 = 7.4$
$\frac{1}{A}\frac{d\sigma}{dt}(t_{min}, A) / \frac{1}{64}\frac{d\sigma}{dt}(t_{min}, 64)$
Be C Al Cu Ag Pb
A
4b
$\sigma_{\rho N} = 31$ mb
$C_0 = 1.18$
$\frac{\gamma_\rho^2}{4\pi} = 1.21 \pm 0.05$
$\chi^2 = 5.2$
$\gamma_\rho^2/4\pi$
4c
$\frac{\gamma_\rho^2}{4\pi} = \left(\frac{93.5 \times f(\sigma_{\rho N}, C_0)}{\frac{d\sigma}{dt}\Big|_{t_{min}}^{(measured)}}\right)\sigma_{\rho N}^2$
Be
C
Cu
Pb
BEST VALUE OF $\frac{\gamma_\rho^2}{4\pi}$, $\sigma_{\rho N}$ FROM THIS EXPERIMENT FOR $C_0 = 1.08$
BEST VALUE OF $\frac{\gamma_\rho^2}{4\pi}$, $\sigma_{\rho N}$ FROM THIS EXPERIMENT FOR $C_0 = 1.18$
$\sigma_{\rho N}$ (mb)
11930A

Fig. 4